



A hybrid of active contour model and convex hull for automated brain tumor segmentation in multimodal MRI

Shiv Naresh Shivhare¹  · Nitin Kumar¹ · Navjot Singh²

Received: 28 December 2018 / Revised: 15 July 2019 / Accepted: 26 July 2019 /
Published online: 17 August 2019
© Springer Science+Business Media, LLC, part of Springer Nature 2019

Abstract

Segmenting tumor automatically in human brain Magnetic Resonance (MR) images is challenging because of uneven, irregular and unstructured size and shape of the tumor. This paper proposes an automated two stage brain tumor segmentation method. In the first stage, coarse estimation of the brain tumor is carried out using convex hull approach. The coarse estimate thus obtained is employed as the initialization for the active contour model applied in the second stage thereby eliminating the need of human intervention. Multiscale Harris energy is estimated at different levels to identify high-energy regions and thereafter constructing convex hull over the selected key-points in order to detect the abnormality in the input MR images. The proposed method is applied to 2-d axial images of fluid attenuated inversion recovery (FLAIR) and post-contrast T1-weighted (T1c) MRI images from the brain tumor segmentation benchmark challenge 2015 (BRATS2015) dataset. Different sub-compartments of the tumor such as enhanced tumor, edema, and necrosis are segmented and in addition combined in the form of tumor core, complete tumor, and enhanced tumor labels. The proposed method is evaluated in terms of Dice Similarity Coefficient (DSC), Sensitivity and Positive Predictive Value (PPV). Average DSC score of 81% for brain tumor core, 92% for complete brain tumor, and 83% for enhanced brain tumor are achieved which is better than several state-of-the-art methods.

Keywords Brain tumor segmentation · Multimodal MRI · Active contour model · Convex hull

✉ Shiv Naresh Shivhare
shiv.naresh@nituk.ac.in

Nitin Kumar
nitin@nituk.ac.in

Navjot Singh
navjot.singh.09@gmail.com

¹ National Institute of Technology Uttarakhand, Srinagar, India

² Motilal Nehru National Institute of Technology Allahabad, Allahabad, India

1 Introduction

A leading Indian newspaper, in a report, states that about 40,000-50,000 patients with brain and central nervous system disorders are being diagnosed every year in India only and more than 20% of them are children [24]. Automation in the field of brain tumor segmentation and abnormality detection is much needed to deal with the diagnosis of the growing number of patients of brain tumor around the world. In recent years, researchers have thrown light to this area and investigated various methods for brain tumor segmentation of the most common malignant brain tumor types e.g. Glioblastoma Multiforme (GBM), Meningioma, Astrocytoma etc. [8, 14, 15, 31, 33].

Manual segmentation of brain tumor along with its different subcompartments from brain images is at par excellence. Researchers from both technological as well as medical fields are attempting to make this task fully automated and have suggested several methods for the same. MR Imaging technology is an essential tool in the process of investigating abnormality in the human brain. Multimodal MRI images are acquired in various radio frequency pulse sequences in which T1 images, post-contrast T1 images, T2 images, and T2 image with fluid-attenuated inversion recovery are widely used for brain image analysis and tumor diagnosis [14]. Figure 1 shows the multimodal MRI sequences with segmented tumor and its sub-compartments of a glioma (a grade-IV brain tumor type) patient taken from BRATS2015 dataset [29].

Methods developed for brain tumor segmentation are broadly divided in two categories [31] i.e. Generative, and Discriminative. Generative methods are based on probabilistic models which constitute anatomical and domain specific cues to segment and detect the presence of tumor with its size and shape. Generative models generally work on the basis of different brain tissue features and spatial characteristics [1, 11, 32, 39]. On the other hand, discriminative methods perform segmentation by setting the accordance between image features and annotated segmentation labels without having any prior domain-specific knowledge. Discriminative methods usually require a manually labelled training data to learn various patterns of tumorous and healthy brain tissues [7, 20, 30, 40]. We have investigated various state-of-the-art methods developed to detect and segment abnormality in brain MR images. The summary of few popular methods is presented in Table 1. In the past, various researchers have suggested numerous methods to detect and segment the tumor in brain MR images and have given a finer classification of segmentation methods depending on the nature of algorithms and approaches used. The most popular conventional methods are region-based, edge and gradient-based, pixel classification and clustering-based methods. Groups of similar and connected pixels are also called regions which satisfy specific characteristics.

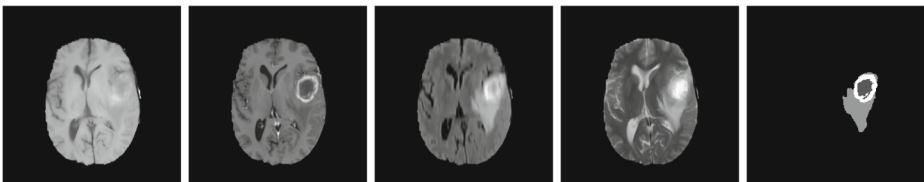


Fig. 1 An axial slice of a high-grade glioma (HGG) subject from BRATS2015 training dataset [29]. From left to right: T1 image, post-contrast T1 image, T2 image with fluid-attenuated inversion recovery, T2 image and ground truth

Table 1 Summary of state-of-the-art methods. [FCM - Fuzzy C-means, DCT - Discrete Cosine Transform, BWT - Berkeley Wavelet Transform, CNN - Convolutional Neural Network, PCA - Principal component analysis, SVM - Support Vector Machine, ANN - Artificial neural network, ACM - Active Contour Model, GLCM - Gray Level Co-occurrence Matrix, LBP - Local Binary Pattern, PM - Percent Match, SI - Similarity Index]

Author(s) (year)	Methodology	Limitation	Performance
Fletcher et al. [16] Kim et al. [28]	Knowledge-based FCM Region growing and clustering	segmenting CSF is challenging. Abnormal tissue detection and segmentation may be difficult due to the limited use of MR modality.	79.2% (PM) –
Prastawa et al. [39]	Knowledge-based generative model with outlier detection	Performance in heterogeneous types such as high-grade gliomas needs attention.	80% (Overlap)
Corso et al. [11]	Generative model with Weighted aggregation	Local contextual cue results in several failure cases.	0.70 (Jaccard)
Menze et al. [32]	Generative model with lesion class	Performance score varies a lot among selected subjects.	0.40-0.80 (Dice)
Bauer et al. [7]	SVM with Hierarchical CRF	Method performs poor while detecting tumor sub-regions.	0.77-0.84 (Dice)
Hsieh et al. [25]	Region growing and FCM clustering	Edema tumor region is undetected.	87% (PM)
Hamamci et al. [20]	Cellular Automata based segmentation	Performance in low- contrast images face challenges.	0.8-0.90 (Dice)
Sachdeva et al. [42, 43]	Content-based ACM with PCA and ANN	Parametric ACM segments whole tumor region while its labels cannot be detected.	85% (Accuracy)
Agn et al. [1]	Generative model	The method takes long time to produce results on a subject.	0.77 (Dice)
Lun et al. [30]	Deep CNN	Performance is relatively lower than state-of-the-art methods.	0.75 (Dice)
Nabizadeh et al. [35]	Texture-based and contour-based model	Parts of the tumor are not segmented.	0.83-0.92 (SI)
Bahadure et al. [5]	Watershed, FCM, DCT and BWT	Various parts of tumor cannot be separated.	0.93 (Dice)
N. Gupta et al. [19]	Ensemble classifier with LBP and GLCM texture features	Tumor segmentation time is not reported.	97% (Accuracy)

Brain lesion structures are partitioned in the form of separate regions of homogeneous tissues while segmenting brain image. Kim et al. [28] adopted region growing approach with clustering techniques for segmenting a medical image of the PET (Positron Emission

Tomography) modality and obtained significant qualitative results. In a similar work, Hsieh et al. [25] implemented the region growing and splitting technique in association with fuzzy c means algorithm and segmented the complete tumor core from T1 and T2 MR images of Meningioma (a malignant brain tumor type) patients. Recently, Bahadure et al. [5] presented a comparative study to detect brain tumor areas using genetic algorithm. Agn et al. [1] suggested a generative segmentation method and predicted brain tumor region using a pre-existing probabilistic model based on convolutional neural network. Many researchers have been using edge-based and gradient-based techniques for the purpose of detecting overall brain tumor region by identifying its boundaries with the help of edge and gradient features [35, 42].

In addition to the conventional approaches, researchers are nowadays adopting advanced techniques like model-based segmentation and multivariate segmentation [40]. Active contour model a.k.a. snake [27] is deformable model which is employed to detect useful information in medical images. In active contour models, a spline under the influence of certain forces is initialized which moves towards an object of interest and delineate its outline. Sachdeva et al. [42] proposed a content-based active contour model using the intensity and texture features and segmented the complete tumor region. They have extended their previous model [43] by selecting multiple features using ANN and PCA to classify six brain tumor types. Using the similar concept, Banday et al. [6] calculated volume of segmented complete tumor. Active contour models are adopted in many recent research works [22, 35, 40, 49] which discuss the snake energy minimization and reported significant results in terms of complete tumor only. However, segmentation of various tumor sub-compartments with active contour models still requires improvement. Moreover, Ren et al. [41] introduced superpixel-based segmentation approach by exploiting the concepts of graph-based [20] and region-based methods. The same approach was also adapted in research works [9, 17, 46]. Shivhare et al. [45] detected brain tumor and segmented tumor core region by utilizing contrast-enhanced T1-weighted MR images by exploiting parameter free k-means clustering algorithm. In another work, Shivhare et al. [44] detected complete brain tumor in FLAIR MR images using superpixel-based manifold ranking approach. In a recent work [48] segmented brain tumor from MRI images primarily based on kernel dictionary learning technique in association with statistical and texture feature extraction. Recently many researchers have moved towards deep machine learning based methods for brain image analysis and tumor segmentation to achieve better performance [19, 23, 26, 30, 37, 38, 50, 51].

Computer-aided diagnosis plays a significant role to assist radiologists and physicians in analyzing medical images [3]. Several researchers have implemented various techniques for brain image diagnosis and analysis from time to time. There is still room for improvement in segmentation accuracy and computation time. Brain tumor and its classes can be considered as objects which possess certain features such as intensity, texture, spatial coordinates, etc [2, 4]. However, in this work, gray-scale intensity values are considered as the local features of brain images. This paper proposes a two-stage method for automated brain tumor segmentation. In the first stage, the coarse tumor region is detected using convex hull. In the second stage, the detected region is refined to a finer level by implementing an active contour model. The output from the first stage is used as the input for the second stage. The tumor segmentation method is executed twice for each patient, one on T1c modality and another on FLAIR modality.

Several significant drawbacks of the current literature have been resolved by our method. The performance obtained in terms of DSC shows that the tumor labels segmented are significantly close to the ground truth. Active contour model efficiently segments the

abnormal brain tissues by fitting the initialized convex hull to the desired object boundaries by applying certain internal and external forces. Our method takes advantages of local gray-scale features of FLAIR and T1c MRI images and segments the abnormal or tumorous brain tissues in the form of complete brain tumor, brain tumor core and enhanced brain tumor by partitioning edema, enhancing tumor and necrosis components. Many current literature methods fail to segment the brain tumor in the form of specific components. The reason for selecting T1c and FLAIR MR modalities is to utilize the visual traits of the same in the advent of brain tissues. T1c MR modality is acquired after injecting Gad chemical agent to the patient. The major advantage of T1c modality is that it highlights enhancing tumor boundary between the edema and brain tumor core. FLAIR pulse sequence shows hyper-intense tumorous brain tissues by way of suppressing CSF inside ventricles. FLAIR modality is the most suitable to come across complete tumor area. Our method detects three labels of the tumor. Complete brain tumor and edema are detected by using FLAIR modality image while enhanced brain tumor is detected by exploiting T1c modality. The computational complexity of the brain tumor segmentation is another challenging issue among the current state-of-the-art methods. Our method tries to resolve this issue by detecting the complete tumor in 8 seconds and various tumor labels in 15 seconds in one 2-D slice image which is computationally faster than several popular existing methods. The method achieves this segmentation speed by mainly two reasons: (i) by removing unwanted and healthy brain tissues using threshold method and (ii) by constructing the convex hull over selected key-points as a rough estimation of tumor region. This convex hull is utilized to automatically initialize the active contour model instead of drawing a curve manually.

The main contribution of the paper is threefold:

1. A two-step method to identify and segment the tumor region in FLAIR and T1c brain MR images is proposed. In the first step, overall brain tissues that possess the tumorous properties are extracted in the form of high energy key-points by exploiting the multi-scale Harris feature extractor. In the second step, a convex hull is constructed over the extracted key-points which surround the rough estimation obtained in the first step. To the best of our knowledge, convex hull and Harris feature extractor function have not been used in literature to detect and segment brain tumor in MR images.
2. Active contour model in its original form is not fully automated and requires manual intervention to provide the initial curve. By applying the previously constructed convex hull to active contour model, we not only incorporate automation but also remove the healthy or normal brain tissues in advance and allow active contour model to process only with selected region of interest (ROI).
3. The proposed method segments a brain MR image into three tumor sub-regions *viz.* (i) Complete brain tumor (ii) Brain tumor core and (iii) Enhanced brain tumor in 15 seconds for one 2-D slice which is computationally faster than several popular existing methods.

The remainder of this paper is structured as follows. Section 2 describes the proposed method for brain tumor identification and how does it segments the tumor sub-regions. Section 3 presents the quantitative and qualitative results on a benchmark dataset. In the end, conclusion and future works are stated in Section 4.

2 Proposed model

Automated brain tumor segmentation model(s) which perform well with respect to both the segmentation accuracy and computation time is yet to be developed due to the uneven

and irregular shape of tumor lesion. Here, we have made an attempt to segment various parts of tumor lesion in a fully automated way by exploiting the concept of convex hull and active contour model. The flowchart of the model consisting of two modules, is shown in the Fig. 2. The first module comprises of the key points detection by exploiting multi-scale Harris function on the preprocessed multimodal MRI image. A convex hull is constructed based on the detected key points. In the second module, a well known region-based active contour model [10] is employed by initializing over the pre-constructed convex hull. The complete tumor region is detected through processing FLAIR MR image and at the same time tumor core and necrosis regions are segmented by processing T1c MR image for the same 2D slice of the corresponding subject as shown in Fig. 2. Finally all the three segmented tumor regions are combined. Figure 2 delineates the segmented enhanced tumor, edema, and necrosis regions in the yellow, green, and red colors respectively. The segmented results of the suggested method are compared with the available ground truth for complete brain tumor, brain tumor core and enhanced brain tumor.

2.1 Preprocessing

Our proposed segmentation model uses two levels of preprocessing. The primary level of preprocessing includes registration and skull-stripping which is previously done in the BRATS dataset. Registration is performed with respect to T1c MRI sequence to apply homogeneity in other MRI sequences due to the fact that T1c modality often possesses the greatest spatial resolution. Thereafter, images are re-sampled with 1 mm of isotropic resolution by exploiting the linear interpolator.

In the secondary level of preprocessing, pixels representing healthy tissues are removed using threshold method. Based on the characteristics of the flair and T1c modality, tumor or abnormality appears bright as compared to the healthy brain tissues. Adopting the same fact, multiple threshold values are applied in MR images and F-score of the complete tumor or whole tumor is computed and compared to the ground truth. The pixels having greater than threshold values are selected and thereafter the mean value of all the selected pixels' intensity is used to remove unwanted pixels. Pixels with intensity value less than this

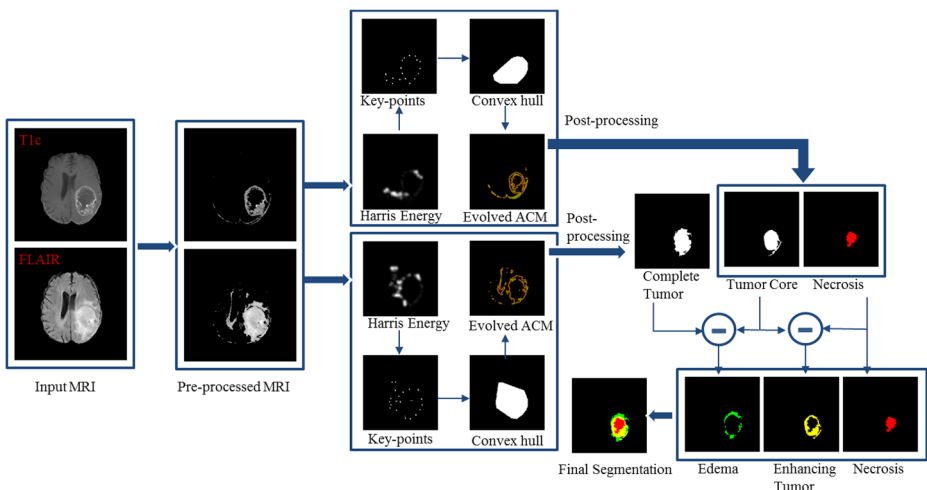


Fig. 2 Flowchart of the proposed model

mean value are removed as they do not possess any significant tumorous information in the image. Experiments are performed on the images and threshold 10 is found as optimal when compared with the F-scores obtained after applying other thresholds as shown in Fig. 3. The preprocessed 2-D images of FLAIR and T1c modalities of few cases are shown in Fig. 4. Case number with corresponding slice number(after underscore symbol) is shown in each row.

2.2 Key-points energy estimation

The fundamental idea behind the key-point generation is to identify the high-energy regions in the image. These high-energy regions can be further recognized by moving a local window in each pixel's neighborhood and selecting the image pixels which differ in terms of intensity values. The image region, *flat* have the least energy whose pixels intensity is almost similar than that of moving the window. The regions *edge* and *corner* are considered as the high-energy regions for containing the pixels that possess significant change in intensity values while moving the local window in various directions. Harris and Stephens [21] introduced a method to detect salient objects in images by detecting and combining the edge and corner points which contain the maximum amount of information related to structure and shape of the objects. A local auto-correlation function is defined by a symmetric matrix \mathbf{M} whose elements and eigenvalues (λ_1 and λ_2) are utilized to extract the needed information.

$$M = w * \begin{bmatrix} X^2 & XY \\ XY & Y^2 \end{bmatrix} \quad (1)$$

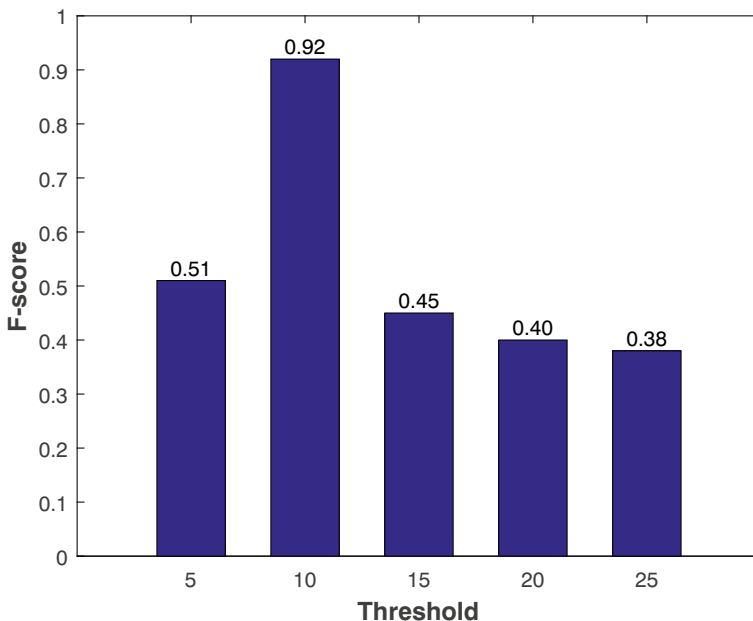


Fig. 3 Comparison of F-scores obtained at multiple thresholds

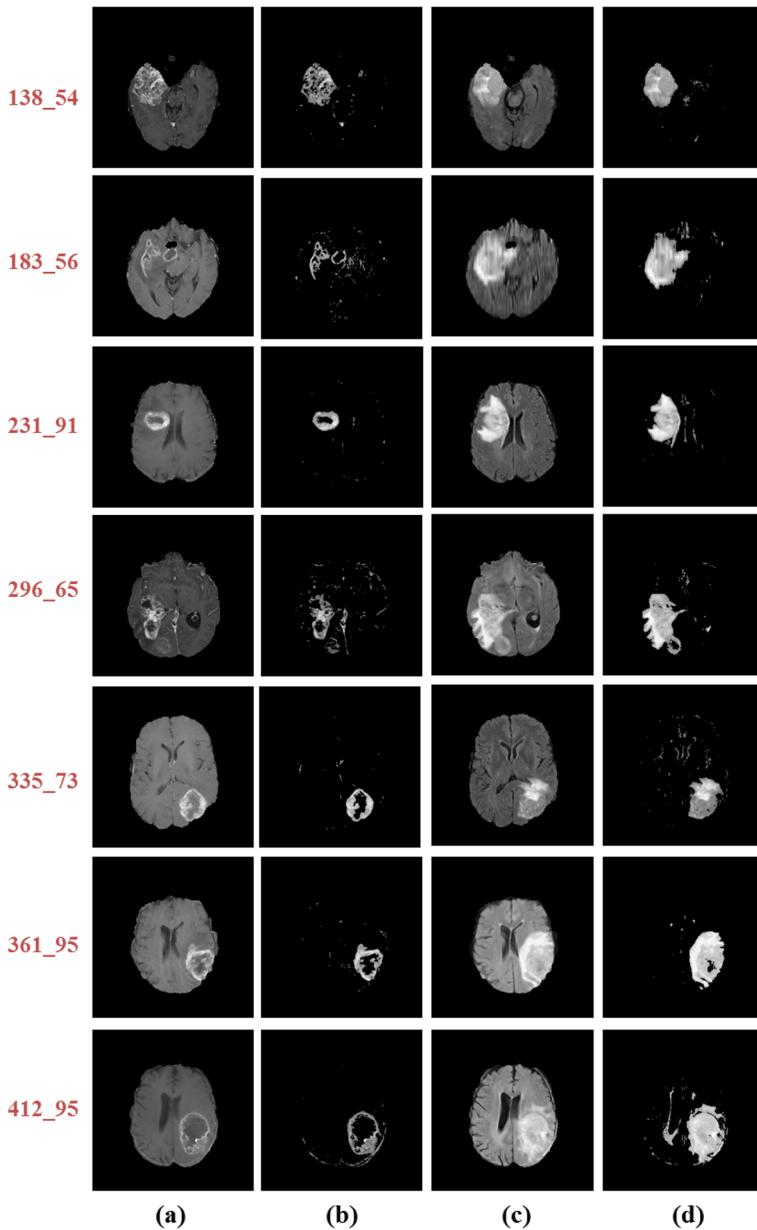


Fig. 4 Preprocessing. **a** T1c MRI modality. **b** Preprocessed T1c image. **c** FLAIR MRI modality. **d** Preprocessed FLAIR image

where w represents the local Gaussian window and X and Y represent first gradients of input image in case of a small shift.

A pixel is identified as *edge* if one eigenvalue is very small, another is comparatively very large and identified as *corner* if eigenvalues are similar and large. Trace and determinant of

the matrix M are utilized to speed-up the computation and measure the response function R for corner regions as per the following equation.

$$R = Det(M) - k * Tr(M)^2 \quad (2)$$

Multiscale Harris energy As observed from the human vision system, human eyes perceive a scene or matter by visualizing its structure, color, size, and dimensions. This visualization is carried out by manifold scales of receptive field available in the anatomy of the human visual system. The finer level cues in the form of abnormality of the brain MR images are obtained based on the above consideration. To compute multiscale Harris energy, Gaussian smoothing filter is applied at the multiple levels in the pyramid structure for each T1c and FLAIR MR image as per the following equation:

$$I^{k+1} = Scaling(I^k \times W_{5 \times 5}) \quad (3)$$

where I represents the input MR image, I^k represents the scaled image at the k^{th} level. Value of k varies from 0 to 5 which shows that Gaussian smoothing filter is applied up to 6 levels. $W_{5 \times 5}$ Gaussian kernel window is used for smoothing operation. Scaling is the function in which the smoothed images are reduced by 2 rows and 2 columns in each level. Multiscale Harris energy is obtained by combining all the scaled images obtained at each level as suggested by [21]:

$$MultiHarris(R) = \sum_{k=0}^5 R^k \quad (4)$$

where R is the response function as determined from (2) and represents the Harris energy in a given input MR image. The accumulated energy due to multiscale Harris function in T1c and FLAIR MR images is shown in Fig. 5b and f respectively.

2.3 Convex hull construction

Brain tumor segmentation is targeted to segment out various sub-compartments of abnormal brain tissues a.k.a. *tumor*, however, the number of abnormal brain tissues are much less than that of normal or healthy brain tissues in any MRI modality. A polygon containing a set of vertices is known as convex hull if the polygon is smallest and every line connecting two vertices lies inside the polygon. Convex hull can be used as a rough estimation to separate out the required affected portion and abnormal brain tissues from most of the healthy tissues for further processing. The multiscale Harris energy obtained in the previous step is used to construct the convex hull which represents and encloses the maximum and significant amount of information related to abnormal brain tissues. Key points of an object are the radial points which acquire the maximum amount of energy. In our experiments, key points are calculated by selecting the highest energy pixel in its 9×9 neighborhood as defined formally in the (5) and Fig. 5 shows the convex hull constructed over the calculated keypoints.

$$\kappa = \{i; \forall j \in N_9(i), Energy(i) > Energy(j)\} \quad (5)$$

where set κ contains the pixel i possessing higher energy than the average of the corresponding 9×9 neighbourhood (N_9) pixels. In our experiments, 35 high valued key-points are selected which possess the maximum amount of information.

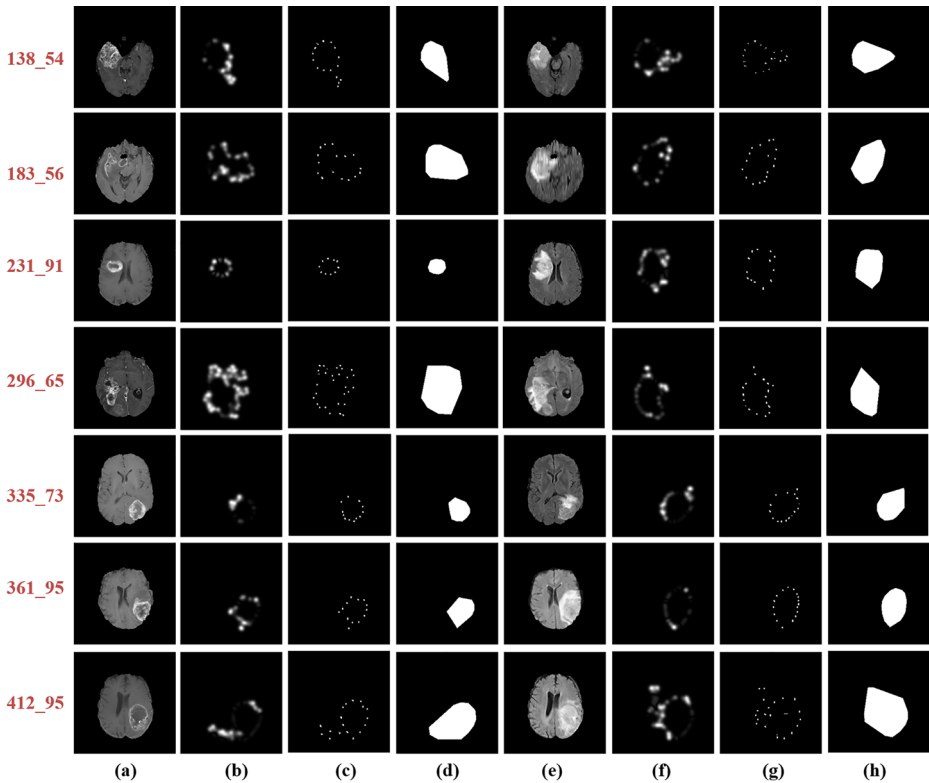


Fig. 5 Convex-hull construction **a** T1c MRI modality. **b** Multi-scale Harris energy in T1c modality. **c** Key-points detected in T1c modality **d** Convex-hull constructed over obtained key-points in T1c modality. **e** FLAIR MRI modality. **f** Multi-scale Harris energy in FLAIR modality. **g** Key-points detected in FLAIR modality. **h** Convex-hull over obtained key-points in FLAIR modality

2.4 Region-based active contour model

After constructing the convex hull from the input image based on the collected key-points, a region-based active contour model is initialized. Most of the active contour models implemented in the state-of-the-art are not fully automated and require user interaction to initialize the model. The proposed method fully initializes the active contour model over the previously constructed convex hull which makes this model fully automated as no user interaction is needed in order to initialize the model. Popular region-based active contour model [10] is adopted which utilizes the statistical information of the image to evolve the snake towards the tumor boundary. Chan and Vese [10] adopted Mumford-shah model [34] and proposed an extended version of active contour model (*snake*) based on the fundamental idea of Kass and Witkin [27] to detect objects of variable shape and size without exploiting the edge and gradient information. The convex hull constructed in the previous module will work as the initial snake which evolve by the effect of internal and external energy components. Internal energy component comprises elastic energy and bending energy which evolves the contour through shrinking and smoothens the contour. At the same time, external energy works on the moving contour and manages the pushing or pulling forces to move the

contour towards the desired object boundary. Therefore the problem of detecting different objects' shape and boundary information is cast as energy minimization problem throughout the evolution of the initialized curve or active contour model. Chan and Vese attempted to solve energy minimization problem as discussed above and derived an energy functional considering the following fitting functional:

$$F_1(C) + F_2(C) = \int_{inside(C)} |I(x, y) - i_1|^2 dx dy + \int_{outside(C)} |I(x, y) - i_2|^2 dx dy \quad (6)$$

where C represents a moving curve, $inside(C)$ exhibits the region inside the curve C and $outside(C)$ shows the region outside of the curve C . Constants i_1 and i_2 denote the mean values of input image I inside and outside the curve respectively. $F_1(C)$ and $F_2(C)$ represents the fitting energy inside and outside the curve C respectively. The above fitting functional can be minimized if curve C evolve exactly at the boundary of the object but not inside and outside of the object. Based on the above assumption and few other significant measures, Chan and Vese derived the energy functional as follows:

$$F(i_1, i_2, C) = \alpha.Length(C) + \beta.Area(inside(C)) + k_1 \int_{inside(C)} |I(x, y) - i_1|^2 dx dy + k_2 \int_{outside(C)} |I(x, y) - i_2|^2 dx dy \quad (7)$$

where $\alpha \geq 0$, $\beta \geq 0$, $k_1, k_2 > 0$ are constants and the required minimization criterion is further represented by the following function:

$$\inf_{i_1, i_2, C} F(i_1, i_2, C)$$

The derived minimization problem is interpreted by the level set formulation [36] in which the evolving curve C is considered as a zero level set of a level set function specifically known as the Lipschitz function $\phi : \Omega \rightarrow \mathfrak{R}$, where Ω is the subset of \mathfrak{R}^2 and the evolving curve C in Ω (Fig. 6).

2.5 Post-processing

In addition to the final evolved curve termed as tumor, few small unwanted background objects also emerged after applying the iterations of active contour model. These background objects a.k.a. holes commonly surrounded by the connected border of foreground pixels [18]. Holes can be removed by applying mathematical morphological operations. Hole filling is an iterative procedure which is defined on the morphological dilation, set intersection and set complement operations based on a symmetrical structuring element. The algorithm converges when there is no change in the results of two successive iterations. Therefore, morphological hole filling operation is applied to refine the segmented tumor as part of post-processing for both the T1c and FLAIR MR images of each case. The

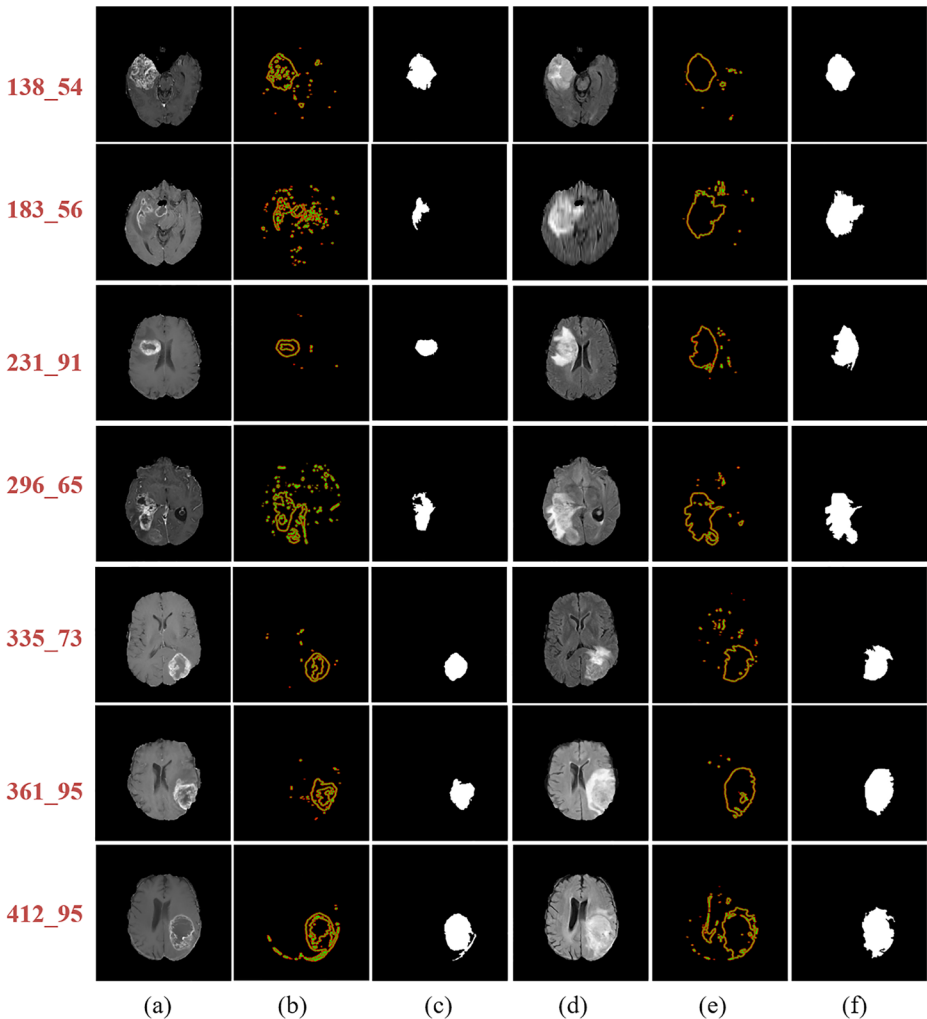


Fig. 6 Active contour evolution. **a** T1c MRI modality. **b** Active contour evolved from T1c modality. **c** Region obtained after post-processing active contour. **d** Post-processed image after performing morphological operations. **e** Active contour evolved from FLAIR modality

experimental results of the proposed method demonstrate that the performance is increased slightly by using morphological post-processing.

3 Experimental results and discussion

The method is evaluated both quantitatively and qualitatively on the publicly available BRATS [29] dataset. All the experiments are performed in the HP workstation over the Windows 10, 64-bit OS with Intel(R) Xeon(R) processor having 2.4 GHz and 16GB of RAM.

3.1 Dataset

BRATS [29] provides a publicly available¹ benchmark dataset containing 220 real MR images of high-grade glioma (HGG) subjects. The 3D MR images are available in four modalities T1 image, post-contrast T1 image (T1c), T2 image and FLAIR. All the scans are acquired under the magnetic field of 1.5T and 3T. T1 image and post-contrast T1 image (T1c) sequences are acquired with 1 to 6 mm of slice thickness whereas T2 and FLAIR image sequences are acquired with 2 to 6 mm of slice thickness. All the MR scans are skull stripped to ensure the anonymity of the subjects and rigidly co-registered with T1c MRI sequence.

Brain tumor in various high-grade glioma patients is typically segmented in *edema* (swelling around the tumorous tissues, also considered as the tumor part), *enhanced brain tumor* (high contrast tumor tissues visible especially after applying a chemical agent Gadolinium while acquiring MRI), *non-enhanced brain tumor* and *necrosis or dead brain tissues*. According to BRATS challenge benchmark [31], the performance of segmentation models can be evaluated in terms of following three tumor labels:

1. Complete Tumor: Combination of all segmented tumor parts i.e. (edema + enhanced brain tumor + non-enhanced brain tumor + necrosis).
2. Tumor Core: Complete brain tumor excluding edema i.e. (enhanced brain tumor + non-enhanced brain tumor + necrosis).
3. Enhancing Tumor: Only segmented enhanced brain tumor.

Probability sampling or random sampling is popular as one of the best sampling methods which is used to choose a sample from a finite dataset. Probability sampling ensures that each possible sample in our case each patient from the dataset has an equal probability of being chosen. In our experiments, a type of probability sampling i.e. cluster sampling is adopted. According to cluster sampling, we have divided all 220 cases (subjects) of the dataset into 11 clusters where each cluster contains 20 subjects. In this way, the method is implemented on the 22 patients of the dataset (i.e. 2 randomly chosen subjects from each cluster).

3.2 Qualitative evaluation

The visual results of a few of the selected images are shown in Fig. 7. The first and second column of images represents the slices of T1c and FLAIR modalities of some patients from the dataset. The slices number of the modality is also shown on the left of T1c modality. The third column shows the edema tumor type detected by the proposed method and is shown in green color. Next two columns delineate the necrosis and enhanced brain tumor regions of the corresponding image slices as shown in red and yellow color respectively. The combined tumor detection result is shown in the second last column while the ground truth is of the corresponding slices are given in the last column. The visual results suggest that the method performs favorable while detecting and segmenting the different brain tumor regions.

3.3 Quantitative evaluation

The quantitative performance of the method is evaluated in terms of DSC, Sensitivity and PPV along with the computation time. DSC [13] give the measure of similarity or the region

¹<https://www.smir.ch/BRATS/Start2015>

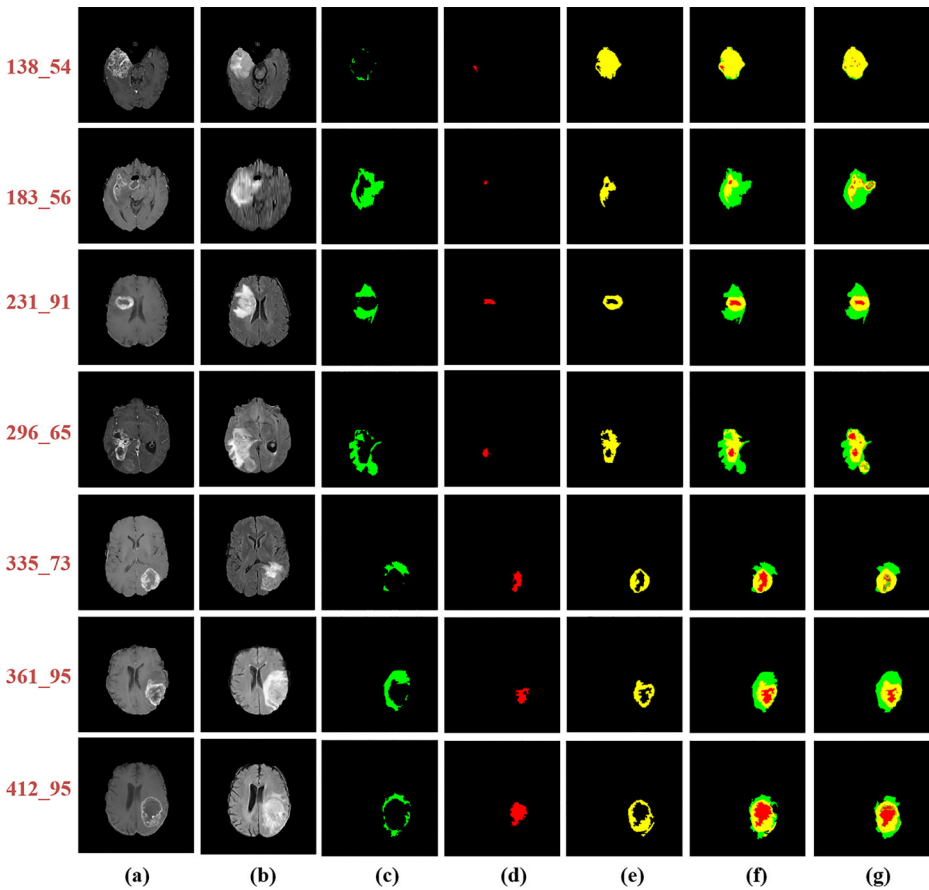


Fig. 7 Qualitative results of proposed method: **a** T1c MRI modality **b** FLAIR MRI modality **c** Segmented edema in green color **d** Segmented necrotic core in red color **e** Segmented enhancing tumor in yellow color **f** Segmented Complete tumor **g** Ground truth

of overlapping between the actual value (ground truth) and the predicted value. Sensitivity is the rate of true positives which shows that with what probability the proposed method correctly predicts the tumorous brain tissues which are tumorous in actual. PPV *a.k.a.* precision is fraction of true positive predictions over all the prediction of the method. These performance measures can be defined as below:

$$DSC = \frac{2 * TP}{(TP + FP) + (TP + FN)} \quad (8)$$

$$Sensitivity = \frac{TP}{TP + FN} \quad (9)$$

$$PPV = \frac{TP}{TP + FP} \quad (10)$$

where FP, TP, FN, and TN represents false positive, true positive, false negative, and true negative respectively.

Table 2 shows the detailed results obtained against each case in terms of performance measures discussed above along with computation time. Performance scores are calculated for predicted complete brain tumor, brain tumor core and enhanced brain tumor. The value of DSC varies between 0.87 (for case 167_0001) and 0.97 (for case 335_0001) with an average of 0.92 (\pm std 0.03) on the 22 selected cases. In the same setting, sensitivity is reported as minimum of 0.80 and maximum of 0.96 for the cases 399_0002 and 183_0001 respectively. The average sensitivity is found to be 0.91 (\pm std 0.04). The high value of sensitivity signifies high true positive rate while predicting the tumorous brain tissues. The average PPV for segmenting the complete tumor is 0.94 (\pm std 0.06) with minimum of 0.79 (for 474_0001) and 0.99 for 5 cases (138_0001, 242_0001, 361_0001, 377_0001 and 399_0002) out of 22 cases. It is interesting to note that all three performance measures computed have value 0.91 or more which is highly encouraging segmentation result.

Edema is also referred to as swelling around real tumorous tissues and consists of the upper most tissues of the tumor. Edema tissues are very less affected and therefore the tissues are not always of similar characteristics. Due to the same, segmenting edema accurately is a challenging task. Tumor core is the combination of all tumorous tissue types

Table 2 Performance scores obtained after applying the proposed method on high-grade glioma images of BRATS2015 training dataset

Case No.	DSC			Sensitivity			PPV			Time (Sec)
	Comp.	Core	Enh.	Comp.	Core	Enh.	Comp.	Core	Enh.	
3_0001	0.94	0.43	0.72	0.94	0.98	0.97	0.94	0.28	0.58	14
15_0001	0.91	0.90	0.85	0.88	0.83	0.78	0.94	0.98	0.95	13
105_0001	0.93	0.67	0.80	0.93	0.62	0.77	0.92	0.85	0.88	19
138_0001	0.97	0.92	0.93	0.95	0.87	0.90	0.99	0.98	0.97	11
167_0001	0.87	0.92	0.94	0.95	0.87	0.94	0.83	0.98	0.94	20
173_0001	0.90	0.65	0.72	0.95	0.60	0.70	0.86	0.73	0.76	13
183_0001	0.96	0.64	0.72	0.96	0.48	0.62	0.95	0.96	0.90	14
184_0001	0.93	0.96	0.96	0.89	0.96	0.95	0.98	0.95	0.96	14
231_0001	0.96	0.90	0.93	0.95	0.83	0.89	0.97	1.00	0.97	22
242_0001	0.91	0.92	0.85	0.84	0.88	0.79	0.99	0.97	0.93	15
274_0001	0.92	0.90	0.89	0.88	0.84	0.81	0.97	0.98	0.98	18
296_0001	0.95	0.79	0.81	0.93	0.72	0.78	0.97	0.91	0.86	15
335_0001	0.97	0.85	0.91	0.96	0.81	0.87	0.98	0.93	0.96	11
361_0001	0.96	0.93	0.91	0.94	0.89	0.86	0.99	0.99	0.98	10
374_0001	0.95	0.66	0.80	0.93	0.51	0.74	0.97	0.95	0.89	16
377_0001	0.91	0.87	0.85	0.84	0.81	0.82	0.99	0.96	0.90	12
399_0002	0.88	0.40	0.31	0.80	0.52	0.62	0.99	0.37	0.22	20
404_0001	0.89	0.88	0.89	0.94	0.87	0.95	0.86	0.89	0.85	17
412_0001	0.95	0.92	0.85	0.95	0.99	0.92	0.94	0.86	0.78	20
430_0001	0.91	0.79	0.83	0.87	0.90	0.92	0.96	0.72	0.76	11
474_0001	0.85	0.94	0.89	0.95	0.91	0.92	0.79	0.97	0.86	18
478_0001	0.90	0.89	0.80	0.89	0.82	0.75	0.92	0.98	0.88	21
Mean	0.92	0.81	0.83	0.91	0.80	0.83	0.94	0.87	0.85	15
Std_dev	0.03	0.16	0.13	0.04	0.15	0.10	0.06	0.19	0.17	3

except to edema which surrounds the tumor core. Hence, tumor core segmentation depends on the precise segmentation of edema. In our results, we have achieved the average DSC of 0.81 (\pm std 0.16) for segmenting the tumor core with minimum 0.40 and maximum 0.93 for the cases 399_0002 and 361_0001 respectively. In terms of sensitivity, we face challenges to segment tumor core but still we obtained satisfactory average score of 0.80 (\pm std 0.15) with minimum 0.48 for case 183_0001 and 0.99 for case 412_0001 as given in Table 2. The average PPV value obtained was 0.87 (\pm std 0.19) while the minimum and maximum values obtained were 0.28 (for 3_0001) and 1.00 (for 231_0001) respectively. As apparent from the experimental results and literature, detection of core tumor is challenging. However, the proposed method is still achieves 0.80 or more value for all the performance measures.

Enhanced brain tumor is a significant part of tumor core which appears bright in T1c MR modality. The proposed method performs efficient segmentation of enhanced brain tumor in terms of average DSC of 0.83 (\pm std 0.13). The average DSC value suffers due to the data of a challenging case 399_002 which is the part of multiple acquisition during its treatment as multiple cases are available for the same subject in the dataset. During the experiments it is observed that it consists of a large amount of heterogeneous brain tissues and due to which our method gives lower segmentation results for this tumor type. The DSC for this case is 0.31 which is minimum on the other hand the maximum DSC is 0.96 for case 184_0001. We have achieved the average sensitivity of 0.83 in which performance on eight cases is more than 0.90 whereas the minimum sensitivity of 0.62 for case 399_002. PPV performs a better segmentation of enhancing tumor with the average accuracy of 0.85. Case 399_002 again affects the overall PPV score of enhancing tumor with the individual score of 0.22 while for other 18 out of 22 cases PPV score is more than 0.85.

The MR image size of each subject is $240 \times 240 \times 155$ which means that the tissues' information of each case is contained in 155 slices out of which about half of the slices contain no information. The proposed method is implemented twice for each case, one for processing T1c modality and another for FLAIR modality. The computation time shown in the Table 2 is the total time needed to detect and segment all the three tumor labels including preprocessing and post-processing. However, if we calculate the time for segmenting complete tumor only, it will become the half of the reported time as the complete tumor is detected by FLAIR modality image only. Our method takes less than 8 seconds to process a slice and around 10 minutes to process all the slices of a subject in order to segment the complete tumor. This cost of the method is due to 1000 iterations of the active contour model but still it is faster than numerous state-of-the-art methods [20, 39, 43].

Figure 8 illustrates the dispersion of the detailed results obtained in terms of performance measures as illustrated in Table 2. Each boxplot depicts the performance score for all the slices of 22 randomly selected patients. The boxplots are shown for complete tumor, tumor core and enhancing tumor. Plus sign in red color represents the outliers. The boxplots suggest that our method generates promising results on most of the subjects in segmenting various tumor labels.

3.4 Comparative analysis

The efficacy of our method is compared with other existing popular methods in Table 3. Figure 9 delineates the DSC scores of different methods in the form of bar chart. The results of other methods are reproduced as reported in literature. It can be easily observed from Fig. 9 that the proposed method outperforms all the compared methods in terms of all the performance measures. The worst performance in terms of brain tumor core and enhanced

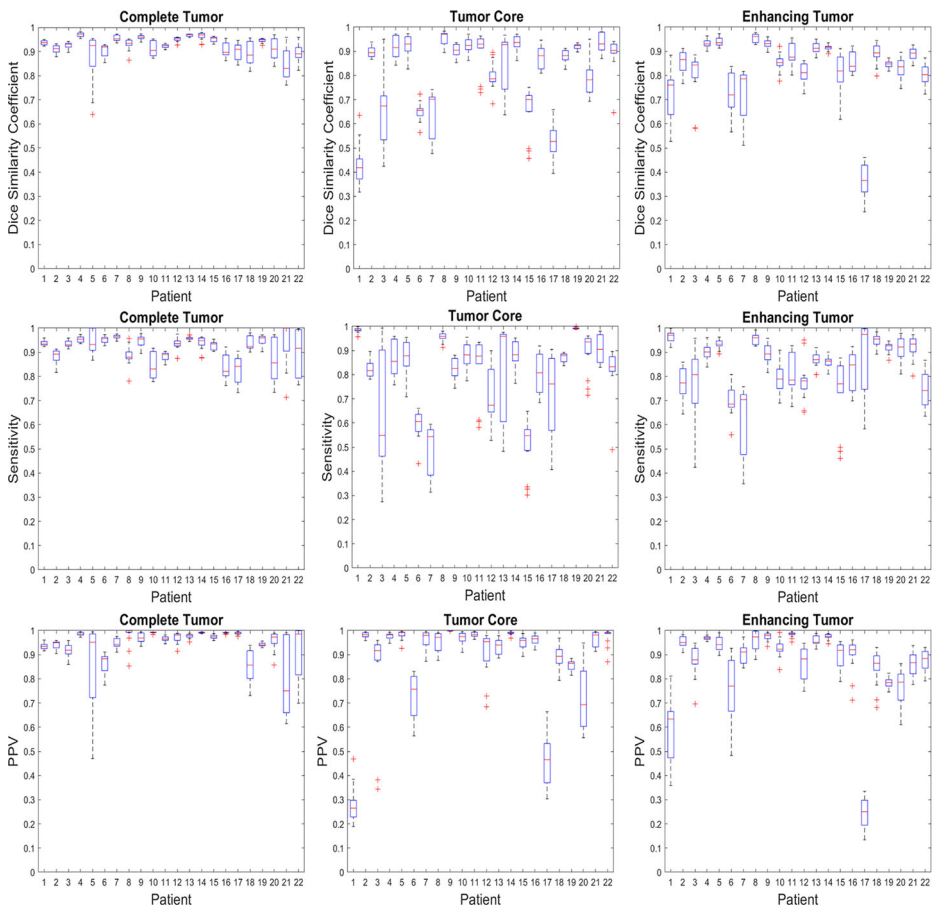


Fig. 8 Boxplots showing the dispersion of the DSC, Sensitivity and PPV for Complete Brain Tumor, Brain Tumor Core and Enhanced Brain Tumor of 22 subjects from the BRATS2015 training data set. “+” indicates outliers

brain tumor is reported by Agn et al. [1] while for complete brain tumor, the worst performance is reported by Lun et al. [30]. Among the compared methods, the performance of Cui et al. [12] is best in terms of DSC but less than our proposed method. For the methods suggested in [1], [50], [47] and [12], the performance in terms of sensitivity and PPV is not reported in literature.

3.5 Discussion

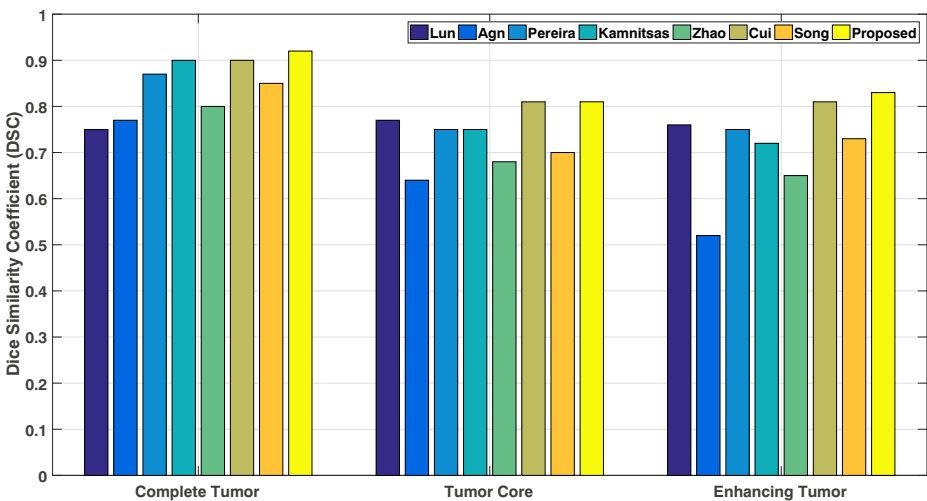
We suggested a fusion of convex hull and active contour model for segmenting different brain tumor labels in multimodal MRI images of glioma patients of BRATS-2015 training dataset. In the experimental setup of region-based active contour model, $\beta = 0$ and $k_1 = k_2 = 1$ is selected for all the images throughout the dataset whereas value of α is not fixed and depends on size and variation in abnormality or tumor. In order to detect many objects of various sizes, small value of α should be applied otherwise empirically large value of α needs to be set. BRATS 2015 dataset mainly contains MR images of Glioma

Table 3 Comparison of our proposed method with the state-of-the-art methods on the HGG cases of BRATS2015 training data set. Symbol “-” used if the performance score is not reported

Methods	DSC			Sensitivity			PPV		
	Comp.	Core	Enh.	Comp.	Core	Enh.	Comp.	Core	Enh.
Lun et al. [30]	0.75	0.77	0.76	0.87	0.85	0.64	0.68	0.71	0.72
Agn et al. [1]	0.77	0.64	0.52	–	–	–	–	–	–
Pereira et al. [38]	0.87	0.75	0.75	0.86	0.79	0.75	0.89	0.76	0.80
Kamnitsas et al. [26]	0.90	0.75	0.72	0.89	0.71	0.74	0.91	0.85	0.75
Zhao et al. [50]	0.80	0.68	0.65	–	–	–	–	–	–
Cui et al. [12]	0.90	0.81	0.81	–	–	–	–	–	–
Song et al. [47]	0.85	0.70	0.73	–	–	–	–	–	–
Proposed Method	0.92	0.81	0.83	0.91	0.80	0.83	0.94	0.87	0.85

The bold symbols represent the highest performance values in each column

tumor type. In most of the Glioma MR images, tumor or abnormal brain tissues often vary in shape, size and number. Due to the same reason, $\alpha = 0.01$ is chosen for all the experiments. The results of our method are compared with the existing methods [1, 26, 30, 38, 47, 50] and its efficacy is exhibited in terms of DSC, Sensitivity and PPV. The detailed identification of enhancing tumor and necrotic core along with the whole tumor lesion using region-based active contour model endorse the capability of the proposed method to facilitate the radiologists. BRATS has provided datasets of brain tumor cases in the form of certain magnetic resonance modalities. Checking the efficacy of a method on different datasets often varies the results and hence the performance on a particular dataset cannot claim for all the datasets. Due to the same reason, we have compared our segmentation results with the methods which have also evaluated on the same dataset. The detailed com-

**Fig. 9** Comparison of DSC of proposed method with other methods

parison in terms of evaluation measures is shown in Table 3 and Fig. 9. Some authors have not reported their method's performance in terms of Sensitivity and PPV. This information is represented with symbol - in Table 3. Several state-of-the-art methods are also investigated with their methodology and the results as shown in Table 1. The limitation of our method is that the non-enhancing tumor cannot be detected by the proposed method due to the fact that intensity values are exploited by our method. The non-enhancing tumor tissues are extremely less in size in most of the cases and possess varying intensity values which get mixed up with edema and enhancing tumor types.

4 Conclusion and future works

In this paper, we propose an efficient brain tumor segmentation model targeted to segment various sub-compartments of the tumor from multimodal MRI images. Segmentation of abnormal brain tissues is initiated by a preprocessing step in which unwanted pixels are removed using thresholding. The method is applied on contrast-enhanced T1-weighted and FLAIR MRI modalities in order to segment brain tumor. Convex hull followed by region-based active contour models are employed for detection and segmentation of tumorous brain tissues. The convex hull is constructed over the key points generated from the multiscale Harris corner detector algorithm and is further used to initialize the active contour model. Tumor core and active tumor are obtained from the T1c modality and FLAIR modality which are helpful in detection of the complete tumor region. Different regions of tumor are detected and thereafter combined to obtain the final segmented tumor in the MRI image. The efficacy of the method was evaluated on the publicly available BRATS 2015 dataset with the DSC score of 81% for brain tumor core, 92% for complete brain tumor, and 83% for segmenting enhanced brain tumor. The measured performance suggest that the method outperformed several popular methods in brain tumor segmentation. In future, we plan to test our method with other real datasets too and to develop new methods for brain tumor detection and segmentation by setting the machine learning environment in conjunction with nature-inspired optimization algorithms.

References

1. Agn M, Puonti O, Law I, af Rosenschöld P, van Leemput K (2015) Brain tumor segmentation by a generative model with a prior on tumor shape. In: Proceeding of the multimodal brain tumor image segmentation challenge, pp 1–4
2. Avola D, Cinque L (2008) Encephalic nmr image analysis by textural interpretation. In: Proceedings of the 2008 ACM symposium on applied computing. ACM, pp 1338–1342
3. Avola D, Cinque L, Di Girolamo M (2011) A novel t-cad framework to support medical image analysis and reconstruction. In: International conference on image analysis and processing. Springer, pp 414–423
4. Avola D, Cinque L, Placidi G (2013) Customized first and second order statistics based operators to support advanced texture analysis of mri images. Computational and mathematical methods in medicine 2013
5. Bahadure NB, Ray AK, Thethi HP (2018) Comparative approach of mri-based brain tumor segmentation and classification using genetic algorithm. J Digit Imaging 31(4):477–489
6. Banday SA, Mir AH (2017) Statistical textural feature and deformable model based brain tumor segmentation and volume estimation. Multimed Tools Appl 76(3):3809–3828
7. Bauer S, Nolte LP, Reyes M (2011) Fully automatic segmentation of brain tumor images using support vector machine classification in combination with hierarchical conditional random field regularization. In: International conference on medical image computing and computer-assisted intervention. Springer, pp 354–361

8. Bauer S, Wiest R, Nolte LP, Reyes M (2013) A survey of mri-based medical image analysis for brain tumor studies. *Phys Med Biol* 58(13):R97
9. Bharath H, Collemann S, Sima D, Van Huffel S (2017) Tumor segmentation from multimodal mri using random forest with superpixel and tensor based feature extraction. In: *International MICCAI brainlesion workshop*. Springer, pp 463–473
10. Chan TF, Vese LA (2001) Active contours without edges. *IEEE Trans Image Process* 10(2):266–277. <https://doi.org/10.1109/83.902291>
11. Corso JJ, Sharon E, Dube S, El-Saden S, Sinha U, Yuille A (2008) Efficient multilevel brain tumor segmentation with integrated bayesian model classification. *IEEE Trans Med Imaging* 27(5):629–640
12. Cui S, Mao L, Jiang J, Liu C, Xiong S (2018) Automatic semantic segmentation of brain gliomas from mri images using a deep cascaded neural network, vol 2018
13. Dice LR (1945) Measures of the amount of ecologic association between species. *Ecol* 26(3):297–302
14. Drevelegas A, Nasel C (2010) *Imaging of brain tumors with histological correlations*. Springer Science & Business Media, New York
15. Dupont C, Betrouni N, Reyns N, Vermandel M (2016) On image segmentation methods applied to glioblastoma: state of art and new trends. *IRBM* 37(3):131–143
16. Fletcher-Heath LM, Hall LO, Goldof DB, Murtagh FR (2001) Automatic segmentation of non-enhancing brain tumors in magnetic resonance images. *Artif Intell Med* 21(1-3):43–63
17. Gong YJ, Zhou Y (2018) Differential evolutionary superpixel segmentation. *IEEE Trans Image Process* 27(3):1390–1404
18. Gonzalez RC, Woods RE (2002) *Digital image processing, Third Edition*. Publishing house of electronics industry
19. Gupta N, Bhatele P, Khanna P (2019) Glioma detection on brain mrIs using texture and morphological features with ensemble learning. *Biomed Signal Process Control* 47:115–125
20. Hamamci A, Kucuk N, Karaman K, Engin K, Unal G (2012) Tumor-cut: segmentation of brain tumors on contrast enhanced mr images for radiosurgery applications. *IEEE Trans Med Imaging* 31(3):790–804
21. Harris C, Stephens M (1988) A combined corner and edge detector. In: *Alvey vision conference*, vol 15. Citeseer, pp 147–151
22. Hasan AM, Meziane F, Aspin R, Jalab HA (2016) Segmentation of brain tumors in mri images using three-dimensional active contour without edge. *Symmetry* 8(11):132
23. Havaei M, Davy A, Warde-Farley D, Biard A, Courville A, Bengio Y, Pal C, Jodoin PM, Larochelle H (2017) Brain tumor segmentation with deep neural networks. *Med Image Anal* 35:18–31
24. Hindu: Over 2,500 indian kids suffer from brain tumour every year www.thehindu.com/sci-tech/health/Over-2500-Indian-kids-suffer-from-brain-tumour-every-year/article14418512.ece (2018). Last Accessed: June 2019
25. Hsieh TM, Liu YM, Liao CC, Xiao F, Chiang IJ, Wong JM (2011) Automatic segmentation of meningioma from non-contrasted brain mri integrating fuzzy clustering and region growing. *BMC Med Inf Decis Making* 11(1):54
26. Kamnitsas K, Ledig C, Newcombe VF, Simpson JP, Kane AD, Menon DK, Rueckert D, Glocker B (2017) Efficient multi-scale 3d cnn with fully connected crf for accurate brain lesion segmentation. *Med Image Anal* 36:61–78
27. Kass M, Witkin A, Terzopoulos D (1988) Snakes: active contour models. *Int J Comput Vis* 1(4):321–331
28. Kim J, Feng DD, Cai TW, Eberl S (2002) Automatic 3d temporal kinetics segmentation of dynamic emission tomography image using adaptive region growing cluster analysis. In: *Nuclear science symposium conference record, 2002 IEEE*, vol 3. IEEE, pp 1580–1583
29. Kistler M, Bonaretti S, Pfahrer M, Niklaus R, Büchler P (2013) The virtual skeleton database: an open access repository for biomedical research and collaboration. *J Med Internet Res* 15(11):e245
30. Lun T, Hsu W (2016) Brain tumor segmentation using deep convolutional neural network. In: *Proceedings of BRATS-MICCAI*
31. Menze BH, Jakab A, Bauer S, Kalpathy-Cramer J, Farahani K, Kirby J, Burren Y, Porz N, Slotboom J, Wiest R et al (2015) The multimodal brain tumor image segmentation benchmark (brats). *IEEE Trans Med Imaging* 34(10):1993–2024
32. Menze BH, Van Leemput K, Lashkari D, Weber MA, Ayache N, Golland P (2010) A generative model for brain tumor segmentation in multi-modal images. In: *International conference on medical image computing and computer-assisted intervention*. Springer, pp 151–159
33. Mohan G, Subashini MM (2018) Mri based medical image analysis: survey on brain tumor grade classification. *Biomed Signal Process Control* 39:139–161
34. Mumford D, Shah J (1989) Optimal approximations by piecewise smooth functions and associated variational problems. *Comm Pure Appl Math* 42(5):577–685

35. Nabizadeh N, Kubat M (2017) Automatic tumor segmentation in single-spectral mri using a texture-based and contour-based algorithm. *Expert Syst Appl* 77:1–10
36. Osher S, Sethian JA (1988) Fronts propagating with curvature-dependent speed: algorithms based on hamilton-jacobi formulations. *J Comput Phys* 79(1):12–49
37. Pereira S, Pinto A, Alves V, Silva C (2016) Brain tumor segmentation using convolutional neural networks in mri images. *IEEE Trans Med Imaging* 35(5):1240–1251
38. Pereira S, Pinto A, Alves V, Silva CA (2015) Deep convolutional neural networks for the segmentation of gliomas in multi-sequence mri. In: *International workshop on brainlesion: glioma, multiple sclerosis, stroke and traumatic brain injuries*. Springer, pp 131–143
39. Prastawa M, Bullitt E, Ho S, Gerig G (2004) A brain tumor segmentation framework based on outlier detection. *Med Image Anal* 8(3):275–283
40. Pratondo A, Chui CK, Ong SH (2017) Integrating machine learning with region-based active contour models in medical image segmentation. *J Vis Commun Image Represent* 43:1–9
41. Ren X, Malik J (2003) Learning a classification model for segmentation. In: *Null*. IEEE, p 10
42. Sachdeva J, Kumar V, Gupta I, Khandelwal N, Ahuja CK (2012) A novel content-based active contour model for brain tumor segmentation. *Magn Reson Imaging* 30(5):694–715
43. Sachdeva J, Kumar V, Gupta I et al (2013) Segmentation, feature extraction, and multiclass brain tumor classification. *J Digit Imaging* 26(6):1141–1150
44. Shivhare SN, Kumar N (2019) Brain tumor detection using manifold ranking in flair mri. In: *International conference on emerging trends in information technology*. Springer in press
45. Shivhare SN, Sharma S, Singh N (2019) An efficient brain tumor detection and segmentation in mri using parameter-free clustering. In: *Machine intelligence and signal analysis*. Springer, pp 485–495
46. Soltaninejad M, Yang G, Lambrou T, Allinson N, Jones TL, Barrick TR, Howe FA, Ye X (2018) Supervised learning based multimodal mri brain tumour segmentation using texture features from supervoxels. *Comput Methods Prog Biomed* 157:69–84
47. Song B, Chou CR, Chen X, Huang A, Liu MC (2016) Anatomy-guided brain tumor segmentation and classification. In: *International workshop on brainlesion: glioma, multiple sclerosis, stroke and traumatic brain injuries*. Springer, pp 162–170
48. Tong J, Zhao Y, Zhang P, Chen L, Jiang L (2019) Mri brain tumor segmentation based on texture features and kernel sparse coding. *Biomed Signal Process Control* 47:387–392
49. Wang K, Ma C (2016) A robust statistics driven volume-scalable active contour for segmenting anatomical structures in volumetric medical images with complex conditions. *Biomed Eng Online* 15(1):39
50. Zhao X, Wu Y, Song G, Li Z, Fan Y, Zhang Y (2016) Brain tumor segmentation using a fully convolutional neural network with conditional random fields. In: *International workshop on brainlesion: glioma, multiple sclerosis, stroke and traumatic brain injuries*. Springer, pp 75–87
51. Zhao X, Wu Y, Song G, Li Z, Zhang Y, Fan Y (2018) A deep learning model integrating fcnn and crfs for brain tumor segmentation. *Med Image Anal* 43:98–111

Publisher's note Springer Nature remains neutral with regard to jurisdictional claims in published maps and institutional affiliations.



Shiv Naresh Shivhare received his M.Tech (Computer Science and Engineering) from Maulana Azad National Institute of Technology, Bhopal, India. He is currently pursuing Ph.D. from National Institute of Technology Uttarakhand, India. His current research areas are computer vision, image processing, pattern recognition, and feature extraction.



Nitin Kumar received his Doctor of Philosophy and Master of Technology from School of Computer and System Sciences, Jawaharlal Nehru University, New Delhi. He is currently working as Assistant Professor at National Institute of Technology, Uttarakhand, India. His current research includes visual attention modeling, pattern recognition, face recognition and image processing.



Navjot Singh is working as an Assistant Professor in Motilal Nehru National Institute of Technology Allahabad, Allahabad, India. He obtained M.Tech. and Ph.D. (Computer Science and Technology) from Jawaharlal Nehru University, New Delhi, India. His current research areas are computer vision, image processing, object detection, pattern recognition, feature extraction and classification.